



Effects of Arctic stratospheric ozone changes on spring precipitation in the northwestern United States

Xuan Ma¹, Fei Xie^{1*}, Jianping Li^{1,2}, Wenshou Tian³, Ruiqiang Ding⁴,
Cheng Sun¹, and Jiankai Zhang³

¹*State Key Laboratory of Earth Surface Processes and Resource Ecology and College of Global
Change and Earth System Science, Beijing Normal University, Beijing, China*

²*Laboratory for Regional Oceanography and Numerical Modeling, Qingdao National Laboratory
for Marine Science and Technology, Qingdao, China*

³*College of Atmospheric Sciences, Lanzhou University, Lanzhou, China*

⁴*State Key Laboratory of Numerical Modeling for Atmospheric Sciences and Geophysical Fluid
Dynamics, Institute of Atmospheric Physics, Chinese Academy of Sciences, Beijing, China*

Submitted as an Article to: *Atmospheric Chemistry and Physics*

7 June 2018

* Corresponding author:

Dr. Fei Xie, Email: xiefei@bnu.edu.cn.



1 **Abstract**

2 Using observations and reanalysis, we find that changes in April precipitation
3 variations in the northwestern US are strongly linked to March Arctic stratospheric
4 ozone (ASO). An increase (decrease) in ASO can result in enhanced (weakened)
5 westerlies in the high and low latitudes of the North Pacific but weakened (enhanced)
6 westerlies in the mid-latitudes. The anomalous circulation over the North Pacific can
7 extend eastward to western North America, facilitating (impeding) the flow of a dry
8 and cold airstream from the middle of North America to the North Pacific and
9 enhancing (weakening) downwelling in the northwestern US, which results in
10 decreased (increased) precipitation there. Model simulations using WACCM4 support
11 the statistical analysis of observations and reanalysis data, and further reveal that the
12 ASO influences circulation anomalies over the northwestern US in two ways.
13 Stratospheric circulation anomalies caused by the ASO changes can propagate
14 downward to the troposphere in the North Pacific and then eastward to influence the
15 strength of the circulation anomalies over the northwestern US. In addition, the ASO
16 changes cause sea surface temperature anomalies over the North Pacific that would
17 cooperate with the ASO changes to modify the circulation anomalies over the
18 northwestern US. Our results suggest that ASO variations could be a useful predictor
19 of spring precipitation changes in the northwestern US; The northwestern US may
20 become dryer in future springs due to ASO recovery.



21 **1. Introduction**

22 Stratospheric circulation anomalies can affect tropospheric climate via chemical–
23 radiative–dynamical feedback processes (Baldwin and Dunkerton, 2001; Graf and
24 Walter, 2005; Cagnazzo and Manzini, 2009; Ineson and Scaife, 2009; Thompson et al.,
25 2011; Reichler et al., 2012; Karpechko et al., 2014; Kidston et al., 2015; Li et al.,
26 2016; Zhang et al., 2016; Wang et al., 2017). Since stratospheric ozone can influence
27 stratospheric circulation via the atmospheric radiation balance (Tung, 1986; Haigh,
28 1994; Ramaswamy et al., 1996; Forster and Shine, 1997; Pawson and Naujokat, 1999;
29 Randel and Wu, 1999, 2007; Solomon, 1999; Labitzke and Naujokat, 2000), the
30 impact of polar ozone on tropospheric climate change has recently received
31 widespread attention.

32 In recent decades, Antarctic stratospheric ozone has decreased dramatically due
33 to the increase in anthropogenic emissions of ozone depleting substances (Solomon,
34 1990, 1999; Ravishankara et al., 1994, 2009). Numerous studies have found that the
35 decreased Antarctic ozone has contributed substantially to climate change in the
36 Southern Hemisphere. The Southern Hemisphere circulation underwent a marked
37 change during the early 21st century, with a slight poleward shift of the westerly jet
38 (Thompson and Solomon, 2002; Lemke et al., 2007). Subsequent studies concluded
39 that Antarctic ozone depletion is responsible for at least 50% of the circulation shift
40 (Lu et al., 2009; Son et al., 2010; McLandress et al., 2011; Polvani et al., 2011; Hu et
41 al., 2013; Gerber and Son, 2014; Waugh et al., 2015). In addition, the poleward
42 displacement of the westerly jet has been linked to an extension of the Hadley cell
43 (Son et al., 2009, 2010; Min and Son, 2013) and variations in mid- to high-latitude
44 precipitation during austral summer; i.e., increased rainfall in the mid-latitudes and
45 reduced rainfall in the high latitudes of the Southern Hemisphere (Thompson et al.,



46 2000, 2011; Marshall, 2003; Archer and Caldeira, 2008; Fogt et al., 2009; Son et al.,
47 2009; Feldstein, 2011; Kang et al., 2011; Polvani et al., 2011). The changes in
48 Antarctic ozone are not only related to the displacement of the westerly jet in the
49 Southern Hemisphere, but also affect its intensity. Thompson and Solomon (2002)
50 argued that Antarctic ozone depletion can also enhance westerly winds via the strong
51 radiative cooling effect and thermal wind relationship. The westerly winds are
52 enhanced from the stratosphere to the mid-latitude troposphere in the case of wave–
53 mean flow interaction (Son et al., 2010; Thompson et al., 2011), thereby accelerating
54 circumpolar currents in the mid-latitudes. The changes in near-surface circumpolar
55 currents restrict the spread of polar cold air to lower latitudes, causing evident climate
56 cooling in the Antarctic interior and warming in the mid-latitudes and subpolar
57 regions. Moreover, changes in subtropical drought, storm tracks and ocean circulation
58 in the Southern Hemisphere are closely related to Antarctic ozone variations (Yin,
59 2005; Russell et al., 2006; Son et al., 2009; Polvani et al., 2011; Bitz and Polvani,
60 2012).

61 The variations in Arctic stratospheric ozone (ASO) in the past five decades are
62 quite different from those of Antarctic stratospheric ozone, as the multi-decadal loss
63 of ASO is much smaller than that of Antarctic stratospheric ozone (WMO, 2011).
64 However, sudden stratospheric warming in the Arctic (Randel, 1988; Charlton and
65 Polvani, 2007; Manney et al., 2011; Manney and Lawrence, 2016) means that the
66 year-to-year variability in ASO has an amplitude equal to or even larger than that of
67 Antarctic stratospheric ozone. Thus, the effect of ASO on Northern Hemisphere
68 climate change has also become a matter of concern.

69 The depletion of ASO can cause circulation anomalies, corresponding to the



70 positive polarity of the Northern Annular Mode (NAM)/North Atlantic Oscillation
71 (NAO) that can affect tropospheric climate and the incidence of extreme weather
72 events. Cheung et al. (2014) used the UK Met Office operational weather forecasting
73 system and Karpechko et al. (2014) used ECHAM5 simulations to investigate the
74 relationship between extreme Arctic ozone anomalies in 2011 and tropospheric
75 climate. Smith and Polvani (2014) used an atmospheric global climate model to reveal
76 a significant influence of ASO changes on tropospheric circulation, surface
77 temperature, and precipitation when the amplitudes of the forcing ASO anomaly in
78 the model are larger than those historically observed. Subsequently, using a fully
79 coupled chemistry–climate model, Calvo et al. (2015) again confirmed that changes in
80 ASO can produce robust anomalies in Northern Hemisphere temperature, wind, and
81 precipitation. Furthermore, the effects of ASO on the Northern Hemisphere climate
82 can be seen in observations. Ivy et al. (2017) presented observational evidence for the
83 relationship between ASO and tropospheric climate, revealing that the maximum
84 daily surface temperature anomalies in spring (March–April) in some regions of the
85 Northern Hemisphere occurred during years with low ASO in March. Xie et al. (2016,
86 2017a, 2017b) demonstrated that the tropical climate can also be affected by ASO.
87 They pointed out that stratospheric circulation anomalies caused by March ASO
88 changes can rapidly extend to the lower troposphere and then propagate horizontally
89 to the North Pacific in about 1 month, influencing the North Pacific sea surface
90 temperature (SST) in April. The induced SST anomalies (Victoria Mode) associated
91 with the circulation anomalies can influence El Niño–Southern Oscillation (ENSO)
92 and tropical rainfall over a timescale of ~20 months.

93 As shown above, a large number of observations and simulations have shown
94 that ASO variations have a significant impact on Northern Hemisphere tropospheric



95 climate, but few studies have focused on regional characteristics. Xie et al. (2018)
96 found that the ASO variations could significantly influence rainfall in the central of
97 China, since the circulation anomalies over the North Pacific caused by ASO
98 variations can extend westward to China. This motivates us to investigate whether the
99 circulation anomalies extend eastward to affect the precipitation in North America. In
100 this study, we find a strong link between ASO and precipitation in the northwestern
101 US in spring. We focus on analyzing the characteristics of the impact of ASO on
102 precipitation in the northwestern US in spring and the associated mechanisms. The
103 remainder of this manuscript is organized as follows. Section 2 describes the data and
104 numerical simulations, and section 3 discusses the relationship between the ASO
105 anomalies and precipitation variations in the northwestern US, as well as the
106 underlying mechanisms. The results of simulations are presented in section 4, and
107 conclusions are given in section 5.

108 **2. Data and simulations**

109 The ASO variations is defined as the Arctic stratospheric ozone averaged over the
110 latitude of 60°–90°N at an altitude of 100–50 hPa after removing the seasonal cycle
111 and trend. Ozone values used in the present analysis are derived from the
112 Stratospheric Water and OzOne Satellite Homogenized (SWOOSH) dataset (Davis et
113 al., 2016), which is a collection of stratospheric ozone and water vapor measurements
114 obtained by multiple limb sounding and solar occultation satellites over the previous
115 30 years. Monthly mean ozone data from SWOOSH (1984–2016) is zonal–mean
116 gridded dataset at a horizontal resolution of 2.5° (latitude: 89°S to 89°N) and vertical
117 pressure range of 31 levels from 316 hPa to 1 hPa. Another set of ozone dataset is
118 taken from Global Ozone Chemistry and Related trace gas Data Records for the
119 Stratosphere (GOZCARDS, 1984–2013) project (Froidevaux et al., 2015) based on



120 high quality data from past missions (e.g., SAGE, HALOE data) and ongoing
121 missions (ACE-FTS and Aura MLS). It is also a zonal–mean dataset with a
122 meridional resolution of 10°, extending from the surface to 0.1 hPa (25 levels).

123 In addition, two sets of global precipitation reanalysis datasets are employed in
124 this study: monthly mean precipitation data constructed by the Global Precipitation
125 Climatology Project (GPCP), which is established by the World Climate Research
126 program (WCRP) in 1986 aiming to observe and estimate the spatial and temporal
127 global precipitation (Huffman et al., 1997), with a resolution of 2.5° latitude/longitude
128 grid for the analysis period 1984–2016; global terrestrial rainfall dataset derived from
129 the Global Precipitation Climatology Centre (GPCC) based on quality-controlled data
130 from 67200 stations world-wide, with a resolution of 1.0° latitude/longitude grid. In
131 addition, SST is taken from the UK Met Office Hadley Centre for Climate Prediction
132 and Research SST (HadSST). Other atmospheric datasets including monthly-mean
133 wind and geopotential height fields for the period 1984–2016 are obtained from the
134 NCEP/Department of Energy (DOE) Reanalysis 2 (NCEP-2), regarding as an updated
135 NCEP/NCAR Reanalysis Project (NCEP-1).

136 We use the Whole Atmosphere Community Climate Model version 4
137 (WACCM4), a part of the National Center for Atmospheric Research’s Community
138 Earth System Model (CESM), version 1.0.6, to investigate precipitation response in
139 the northwestern U.S. to the ASO anomalies. WACCM4 encompasses the Community
140 Atmospheric Model version 4 (CAM4) and as such includes all of its physical
141 parameterizations (Neale et al., 2013). It uses a coupled system made up of four
142 components, namely atmosphere, ocean (specified SST), land, and sea ice (Holland et
143 al., 2012) and has detailed middle–atmosphere chemistry. This improved version of



144 WACCM uses a finite-volume dynamical core, and it extends from the surface to
145 approximately 145 km geometric altitude (66 levels), with a vertical resolution of
146 about 1 km in the tropical tropopause layer and the lower stratosphere. The
147 simulations in the present paper is at a $1.9^\circ \times 2.5^\circ$ horizontal resolution, and do not
148 include interactive chemistry (Garcia et al., 2007). More information can be seen in
149 Marsh et al. (2013). The model's radiation scheme uses these conditions: fixed
150 greenhouse gas (GHG) values, averages of emissions scenario A2 of the
151 Intergovernmental Panel on Climate Change (IPCC) (WMO, 2003) for 1980–2015.
152 The prescribed ozone forcing used in the experiments is a 12-month seasonal cycle
153 averaged over the period 1980–2015 from CMIP5 ensemble mean ozone output. The
154 Quasi Biennial Oscillation (QBO) phase signals with a 28-month fixed cycle are
155 included in WACCM4 as an external forcing for zonal wind.

156 Seven time-slice experiments (R1–R7) are designed to investigate the
157 precipitation changes in the northwestern U.S. due to the ASO anomalies. Details of
158 the seven experiments are given in Table 1. All the experiments are run for 33 years,
159 with the first 3 years excluded for the model spin-up and only the last 30 years are
160 used for analysis.

161 **3. Response of precipitation in the northwestern US to ASO anomalies in** 162 **spring**

163 Since the variations in ASO are most obvious in March due to the Arctic polar vortex
164 rupture (Manney et al., 2011), previous studies have reported that the ASO changes in
165 March have the strongest influence on the Northern Hemisphere (Ivy et al., 2017; Xie
166 et al., 2017a). In addition, these studies pointed out that the changes in ASO affect the
167 tropospheric climate with a lead of about 1–2 months; the relevant mechanisms have



168 been investigated in detail by Xie et al. (2017a). We therefore show in Fig. 1 the
169 correlation coefficients between ASO variations in March from SWOOSH and
170 GOZCARDS data, and precipitation anomalies in April from GPCC and GPCP data
171 over western North America. In all cases in Fig. 1 the March ASO changes are
172 significantly anti-correlated with April precipitation anomalies in the northwestern US
173 (mainly in Washington and Oregon states), implying that positive (negative) spring
174 ASO anomalies are associated with less (more) spring precipitation in the
175 northwestern US. Note that since this kind of feature appears in the northwestern U.S.,
176 the Fig. 1 shows only the west side of North America.

177 The correlation coefficients between March ASO variations and precipitation
178 anomalies (January to December are in the same year) in the northwestern US are
179 shown in Fig. 2. The correlation coefficients between March ASO variations and April
180 precipitation anomalies in the northwestern US are the largest and are significant at
181 the 95% confidence level. Note that the correlation coefficients between March ASO
182 variations and July precipitation anomalies are also significant. The impact of March
183 ASO on the northwestern US in summer and the associated mechanisms are different
184 from those considered in this study (not shown) and will be presented in another paper,
185 but will not be investigated further here. March ASO changes are not significantly
186 correlated with simultaneous (March) precipitation variations (Fig. 2), illustrating that
187 the ASO changes lead precipitation anomalies by about 1 month. Since the results
188 from four sets of observations show a common feature, and SWOOSH and GPCP data
189 span a longer period, only SWOOSH ozone and GPCP precipitation are used in the
190 following analysis.

191 Figure 3 shows the differences between composite anomalies of April



192 precipitation in the northwestern US during positive and negative March ASO
193 anomaly events to further confirm the relationship between March ASO changes and
194 April precipitation anomalies in the northwestern US. The increase (decrease) in
195 March ASO is associated with decreased (increased) April precipitation in the
196 northwestern US. The pattern of the difference in Fig. 3 is consistent with the pattern
197 of the correlation coefficients in Fig. 1. Note that an anomalous signal of precipitation
198 is found in the southwestern US; however, this phenomenon is not significant in Fig.
199 1 and may be an artefact of the composite analysis.

200 The above statistical analysis shows a strong negative correlation between March
201 ASO variations and April precipitation anomalies in the northwestern US, meaning
202 that the ASO can be used to predict changes in spring precipitation in the
203 northwestern US. It may also imply that the northwestern US will become dryer in
204 future springs due to ASO recovery. The process and underlying mechanism that are
205 responsible for the impact of ASO anomalies on precipitation changes need further
206 analysis.

207 Figure 4a, c and e shows the correlation coefficients between March ASO
208 anomalies and April zonal wind variations at 200, 500, and 850 hPa, respectively. The
209 spatial distribution of significant correlation coefficients over the North Pacific
210 exhibits a tripolar mode with a zonal distribution at 200 and 500 hPa; i.e. a positive
211 correlation in the high and low latitudes in the North Pacific and a negative
212 correlation in mid-latitudes. This implies that the increase (decrease) in ASO can
213 result in enhanced (weakened) westerlies in the high and low latitudes of the North
214 Pacific but weakened (enhanced) westerlies in the mid-latitudes. At 850 hPa, the
215 anomalous circulation signal in the low latitudes of the North Pacific has weakened



216 and disappeared. It is evident from Fig. 4 that the anomalous changes in the zonal
217 wind over the North Pacific can extend westward to East Asia. Xie et al. (2018)
218 identified the effect of spring ASO changes on spring precipitation in China. Note that
219 the zonal wind anomalies can also extend eastward to North America, implying a
220 possible influence of spring ASO variations on weather and climate in western North
221 America. Figure 4b, d and f shows the differences between April zonal wind
222 anomalies during positive and negative March ASO anomaly events at 200, 500, and
223 850 hPa, respectively. The spatial distributions of the differences are in good
224 agreement with those of the correlation coefficients between March ASO and April
225 zonal wind variations (Fig. 4a, c and e). Figure 5a, c and e shows the correlation
226 coefficients between March ASO and April geopotential height variations at 200, 500,
227 and 850 hPa, respectively. The differences between April geopotential height
228 anomalies during positive and negative March ASO anomaly events at 200, 500, and
229 850 hPa are shown in Fig. 5b, d and f, respectively. The variations in geopotential
230 height associated with ASO anomalies correspond closely to those of zonal wind.

231 Figures 4 and 5 show that the March ASO anomalies may be linked with
232 anomalous April zonal wind over the North Pacific; i.e., the increase (decrease) in
233 ASO can result in enhanced (weakened) westerlies in the high and low latitudes of the
234 North Pacific but weakened (enhanced) westerlies in the mid-latitudes. It is clear that
235 the weakened (enhanced) westerlies in the mid-latitudes and the enhanced (weakened)
236 westerlies in the low latitudes can extend eastward to the western US. This kind of
237 circulation anomaly corresponds to an anomalous cyclone (anticyclone) in the western
238 US in the middle and upper troposphere, which is likely associated with a strong low
239 (high) pressure system in the middle and upper troposphere and a relatively weak high
240 (low) pressure system in the lower troposphere.



241 To further validate our conjecture regarding the response of the circulation in the
242 western US to ASO changes, we analyze the differences between April horizontal
243 wind anomalies during positive and negative March ASO anomaly events at 200, 500,
244 and 850 hPa (Fig. 6). There is an anomalous cyclone in the southwestern US related
245 to the increase in March ASO. This kind of circulation anomaly over the southwestern
246 US enhances cold and dry airflow from the North American continent to the North
247 Pacific, reducing the water vapor concentration in the air over the northwestern US,
248 and possibly decreasing the local April precipitation. In addition, a strong
249 low-pressure system in the middle and upper troposphere over the western US during
250 positive ASO anomaly events (Fig. 6) suggests downwelling flow in the region.

251 Figure 7 shows a longitude–latitude cross-section of differences between April
252 vertical velocity anomalies averaged over 1000–500 hPa during positive and negative
253 March ASO anomaly events. When the March ASO increases, tropospheric
254 convective activity in the northwestern US (115°–130° W) weakens, corresponding to
255 anomalous downwelling. This situation may also decrease April precipitation in the
256 northwestern US. Figure 7b depicts a longitude–height cross-section of differences
257 between April vertical velocity averaged over 43°–50°N during positive and negative
258 March ASO anomaly events, which further shows that tropospheric convective
259 activity over the northwestern US enhances when the March ASO increases. Based on
260 the above analysis, the circulation anomalies in the northwestern US associated with
261 positive (negative) March ASO anomalies may reduce (increase) the local
262 precipitation in April.

263 **4. Simulations of the effect of ASO variations on precipitation in the** 264 **northwestern US during spring**



265 Using observations and reanalysis data, we investigated the relationship between
266 March ASO and April precipitation in the northwestern US and revealed the
267 underlying mechanisms in section 3. In this section, we use WACCM4 simulations
268 (see section 2) to confirm the above conclusions. First, we check the model
269 performance in simulating precipitation over western North America. Figure 8 shows
270 the April precipitation climatology over the region 95° – 140° W, 30° – 63° N from the
271 control experiment R1 (Table 1) and from GPCP for the period 1995–2005. The
272 model simulates a center of high precipitation over the west coast of North America
273 (Fig. 8a). It is clear that the spatial distribution of the simulated precipitation
274 climatology is similar to that calculated by GPCP (Fig. 8b).

275 Figure 9a displays the differences in April precipitation between experiments R3
276 and R2. The pattern of simulated April precipitation anomalies forced by ASO
277 changes in western North America (Fig. 9a) is nearly opposite to that observed (Fig.
278 3); i.e., the increased March ASO forces an increase in precipitation in the
279 northwestern US. The differences in April zonal wind at 200, 500, and 850 hPa
280 between experiments R3 and R2 are shown in Fig. 9b, c, and d, respectively. The
281 simulated pattern of April zonal wind anomalies in western North America (Fig. 9b, c
282 and d) is also opposite to that observed (Fig. 4). Comparing the global pattern of
283 simulated April zonal wind anomalies with the observations, it is surprising to find
284 that the positions of simulated zonal wind anomalies over the Northeast Pacific and
285 western North America are shifted northward. This results in the simulated
286 precipitation anomalies over western North America also shifting northward, so that a
287 decrease in precipitation on the west coast of Canada in April is found in Fig. 9a. This
288 explains why we find the pattern of simulated April precipitation anomalies in the
289 North America (Fig. 9a) is nearly opposite to that observed (Fig. 3). Figure 9 shows



290 that the results of the model simulation in which we only change the ASO forcing do
291 not reflect the real situation of April precipitation anomalies in the northwestern US,
292 with a shift in position compared with observations. This leads us to consider whether
293 other factors interact with March ozone to influence April precipitation in the
294 northwestern US.

295 Previous studies have found that the North Pacific SST has a significant effect on
296 precipitation in the US (e.g., Namias, 1983; Ting and Wang, 1997; Wang and Ting,
297 2000; Barlow et al., 2001; Lau et al., 2002; Wang et al., 2014). Figure 10a shows the
298 correlation coefficients between regional averaged (43° – 50° N, 115° – 130° W)
299 precipitation anomalies and SST variations in April. Interestingly, the results show
300 that the distribution of correlation coefficients over the North Pacific has a meridional
301 tripole structure, which is referred to as the Victoria Mode SST anomaly pattern. Xie
302 et al. (2017a) reported that the stratospheric circulation anomalies caused by March
303 ASO changes can rapidly extend to the North Pacific over about 1 month, influencing
304 the North Pacific SST and inducing Victoria Mode anomalies. Figure 10b shows the
305 correlation coefficients between March ASO (multiplied by -1) and April SST
306 variations. The pattern in Fig. 10b is in good agreement with that in Fig. 10a. It is
307 further found that removing the Victoria Mode signal from the time series of
308 precipitation in the northwestern US reduces the correlation coefficient between
309 March ASO anomalies and filtered April precipitation variations in the northwestern
310 US to -0.40 (the correlation coefficient is -0.63 for the original time series, see Fig.
311 2), but it remains significant. Figure 10 indicates that the ASO possibly influences
312 precipitation anomalies in the northwestern US in two ways. First, the stratospheric
313 circulation anomalies caused by the ASO changes can propagate downward to the
314 North Pacific troposphere and eastward to influence precipitation over northwestern



315 US. Second, the ASO changes generate SST anomalies over the North Pacific that act
316 as a bridge for ASO to affect precipitation in the northwestern US. The SST
317 anomalies caused by ASO change likely interact with the direct changes in
318 atmospheric circulation driven by the ASO change to jointly influence precipitation in
319 the northwestern US. Experiments R2 and R3 do not include the effects of SST, which
320 may explain why the results of the model simulation in which we only change the
321 ASO forcing do not reflect the observed precipitation anomalies in the northwestern
322 US (Fig. 9).

323 Two sets of experiments (R4 and R5) that include the joint effects of ASO and
324 SST change are added. Details of the experiments are given in Table 1. Figure 11
325 shows the differences in April precipitation and zonal wind between experiments R5
326 and R4. It is clear that the simulated changes in precipitation in the northwestern US
327 (Fig. 11a) are in good agreement with the observed anomalies shown in Fig. 3; i.e.,
328 the increase in March ASO forces a decrease in April precipitation in the northwestern
329 US. In addition, the spatial distributions of simulated zonal wind anomalies (Fig. 11b–
330 d) are consistent with the observations (Fig. 4). Overall, the simulated precipitation
331 and circulation in R4 and R5 are no longer shifted northward and are closer to the
332 observations.

333 To further emphasize the importance of the joint effects of ASO and ASO-related
334 SST anomalies on precipitation in the northwestern US, we investigate whether the
335 spring Victoria Mode-like SST anomalies alone could force the observed
336 precipitation anomalies in the northwestern US. Two sets of experiments are
337 performed here (R6 and R7), in which only April SST anomalies over the North
338 Pacific have been changed (Fig. 12). Details of the experiments are given in Table 1.



339 Figure 13 shows the differences in April precipitation and zonal wind between
340 experiments R7 and R6. The simulated precipitation anomalies over the west coast of
341 the US (Fig. 13a) are much weaker than in the observations (Fig. 3), and the
342 simulated circulation anomalies (Fig. 13b–d) are quite different from those in Fig. 4.
343 This suggests that the ASO-related North Pacific SST anomalies alone cannot force
344 the observed precipitation anomalies in the northwestern US, but that the combined
345 effect of ASO and ASO-related North Pacific SST anomalies is required (Fig. 11).
346 Thus, we have shown that the relationship between March ASO and April
347 precipitation in the northwestern US in the observations and the underlying
348 mechanisms can be verified by WACCM4.

349 **5. Summary and conclusions**

350 Many observations and simulations have shown that ASO variations have a
351 significant impact on Northern Hemisphere tropospheric climate, but few studies have
352 focused on regional characteristics. Using observations, reanalysis datasets, and
353 WACCM4, we have shown that spring ASO changes have a significant effect on April
354 precipitation in the northwestern US (mainly in Washington and Oregon states) with a
355 lead of 1–2 months. When the March ASO is anomalously high (low), April
356 precipitation decreases (increases) in the northwestern US.

357 During positive ASO events, the zonal wind changes over the North Pacific
358 exhibit a tripolar mode with a zonal distribution accompanied by geopotential height
359 anomalies; i.e., enhanced westerlies in the high and low latitudes of the North Pacific,
360 and weakened westerlies in the mid-latitudes. The anomalous wind can extend
361 eastward to North America, causing anomalous circulation in western North America.
362 Such circulation anomalies force an anomalous cyclone in the western US in the



363 middle and upper troposphere, which likely enhances cold and dry airflow from the
364 North American continent to the North Pacific, reducing the water vapor
365 concentration in the air over the northwestern US. At the same time, convection in the
366 northwestern US is weakened. The two processes possibly decrease April
367 precipitation in the northwestern US. When the March ASO is reduced, the effect is
368 just the opposite.

369 The WACCM4 model is used to confirm the statistical results of observations
370 and the reanalysis data. The results of the model simulation in which we only change
371 the ASO forcing do not reflect the observed precipitation anomalies in the
372 northwestern US in April; i.e., the pattern of simulated April precipitation and
373 circulation anomalies in the western North America is opposite to that observed. It is
374 found that SST anomalies over North Pacific caused by ASO changes are likely to
375 interact with ASO changes to jointly influence precipitation in the northwestern US.
376 Thus, the ASO influences precipitation anomalies over the northwestern US in two
377 ways. First, the stratospheric circulation anomalies caused by the ASO change can
378 propagate downward to the North Pacific troposphere and directly influence
379 precipitation over the northwestern US. Second, the ASO changes generate SST
380 anomalies over the North Pacific that act as a bridge, allowing the ASO changes to
381 affect precipitation in the northwestern US.

382 **Acknowledgments.** Funding for this project was provided by the National Natural
383 Science Foundation of China (41575039 and 41630421). We acknowledge ozone
384 datasets from the SWOOSH and GOZCARDS; precipitation from China
385 Meteorological Administration, GPCP and GPCP; Meteorological fields from NCEP2,
386 and WACCM4 from NCAR.



387 **References:**

- 388 Archer, C. L. and Caldeira, K.: Historical trends in the jet streams, *Geophys. Res.*
389 *Lett.*, 35, L08803, doi:10.1029/2008GL033614, 2008.
- 390 Baldwin, M. P. and Dunkerton, T. J.: Stratospheric harbingers of anomalous weather
391 regimes, *Science*, 294, 581–584, doi:10.1126/science.1063315, 2001.
- 392 Barlow, M., Nigam, S., and Berbery, E. H.: ENSO, Pacific decadal variability, and US
393 summertime precipitation, drought, and stream flow, *J. Climate*, 14, 2105–2128,
394 doi:10.1175/1520-0442(2001)014<2105:EPDVAU>2.0.CO;2, 2001.
- 395 Bitz, C. M. and Polvani, L. M.: Antarctic climate response to stratospheric ozone
396 depletion in a fine resolution ocean climate model, *Geophys. Res. Lett.*, 39,
397 L20705, doi:10.1029/2012GL053393, 2012.
- 398 Cagnazzo, C. and Manzini, E.: Impact of the Stratosphere on the Winter Tropospheric
399 Teleconnections between ENSO and the North Atlantic and European Region, *J.*
400 *Climate*, 22, 1223–1238, doi:10.1175/2008JCLI2549.1, 2009.
- 401 Calvo, N., Polvani, L. M., and Solomon, S.: On the surface impact of Arctic
402 stratospheric ozone extremes, *Environ. Res. Lett.*, 10, 094003,
403 doi:10.1088/1748-9326/10/9/094003, 2015.
- 404 Charlton, A. J. and Polvani, L. M.: A new look at stratospheric sudden warmings. Part
405 I: Climatology and modeling benchmarks, *J. Climate*, 20, 449–469,
406 doi:10.1175/JCLI3996.1, 2007.
- 407 Cheung, J. C. H., Haigh, J. D., and Jackson, D. R.: Impact of EOS MLS ozone data on
408 medium-extended range ensemble weather forecasts, *J. Geophys. Res.*, 119,



- 409 9253–9266, doi:10.1002/2014JD021823, 2014.
- 410 Davis, S. M, Rosenlof, K. H., Hassler, B., Hurst, D. F., Read, W. G., Vomel, H.,
411 Selkirk, H., Fujiwara, M., and Damadeo, R.: The Stratospheric Water and
412 Ozone Satellite Homogenized (SWOOSH) database: a long-term database for
413 climate studies, *Earth Syst Sci Data*, 8, 461–490, doi:10.5194/essd-8-461-2016,
414 2016.
- 415 Feldstein, S. B.: Subtropical Rainfall and the Antarctic Ozone Hole, *Science*, 332,
416 925–926, doi:10.1126/science.1206834, 2011.
- 417 Fogt, R. L., Perlwitz, J., Monaghan, A. J., Bromwich, D. H., Jones, J. M., and
418 Marshall, G. J.: Historical SAM variability. Part II: Twentieth-century variability
419 and trends from reconstructions, observations, and the IPCC AR4 models, *J.*
420 *Climate*, 22, 5346–5365, doi:10.1175/2009JCLI2786.1, 2009.
- 421 Forster, P. M. D. and Shine, K. P.: Radiative forcing and temperature trends from
422 stratospheric ozone changes, *J. Geophys. Res.*, 102, 10841–10855,
423 doi:10.1029/96JD03510, 1997.
- 424 Froidevaux, L., Anderson, J., Wang, H.-J., Fuller, R. A., Schwartz, M. J., Santee, M.
425 L., Livesey, N. J., Pumphrey, H. C., Bernath, P. F., Russell III, J. M., and
426 McCormick, M. P.: Global Ozone Chemistry And Related trace gas Data records
427 for the Stratosphere (GOZCARDS): methodology and sample results with a
428 focus on HCl, H₂O, and O₃, *Atmos. Chem. Phys.*, 15, 10471–10507,
429 doi:10.5194/acp-15-10471-2015, 2015.
- 430 Garcia, R. R., Marsh, D. R., Kinnison, D. E., Boville, B. A., and Sassi, F.: Simulation



- 431 of secular trends in the middle atmosphere, 1950–2003, *J. Geophys. Res.*, 112,
432 D09301, doi:10.1029/2006JD007485, 2007.
- 433 Gerber, E. P. and Son, S. W.: Quantifying the Summertime Response of the Austral Jet
434 Stream and Hadley Cell to Stratospheric Ozone and Greenhouse Gases, *J.*
435 *Climate*, 27, 5538–5559, doi:10.1175/JCLI-D-13-00539.1, 2014.
- 436 Graf, H. F. and Walter, K.: Polar vortex controls coupling of North Atlantic Ocean and
437 atmosphere, *Geophys. Res. Lett.*, 32, L01704, doi:10.1029/2004GL020664,
438 2005.
- 439 Haigh, J. D.: The Role of Stratospheric Ozone in Modulating the Solar Radiative
440 Forcing of Climate, *Nature*, 370, 544–546, doi:10.1038/370544a0, 1994.
- 441 Holland, M. M., Bailey, D. A., Briegleb, B. P., Light, B., and Hunke, E.: Improved
442 Sea Ice Shortwave Radiation Physics in CCSM4: The Impact of Melt Ponds and
443 Aerosols on Arctic Sea Ice, *J. Climate*, 25, 1413–1430,
444 doi:10.1175/JCLI-D-11-00078.1, 2012.
- 445 Hu, Y., Tao, L., and Liu, J.: Poleward expansion of the Hadley circulation in CMIP5
446 simulations, *Adv. Atmos. Sci.*, 30, 790–795, doi:10.1007/s00376-012-2187-4,
447 2013.
- 448 Huffman, G. J., Adler, R. F., Arkin, P., Chang, A., Ferraro, R., Gruber, A., Janowiak, J.,
449 McNab, A., Rudolf, B., and Schneider, U.: The Global Precipitation Climatology
450 Project (GPCP) Combined Precipitation Dataset, *B. Am. Meteorol. Soc.*, 78, 5–
451 20, doi:10.1175/1520-0477(1997)078<0005:TGPCPG>2.0.Co;2, 1997.
- 452 Ineson, S. and Scaife, A. A.: The role of the stratosphere in the European climate



- 453 response to El Nino, *Nat. Geosci.*, 2, 32–36, doi:10.1038/NGEO381, 2009.
- 454 Ivy, D. J., Solomon, S., Calvo, N., and Thompson, D. W.: Observed connections of
455 Arctic stratospheric ozone extremes to Northern Hemisphere surface climate,
456 *Environ. Res. Lett.*, 12, 024004, doi:10.1088/1748-9326/aa57a4, 2017.
- 457 Kang, S. M., Polvani, L. M., Fyfe, J. C., and Sigmond, M.: Impact of Polar Ozone
458 Depletion on Subtropical Precipitation, *Science*, 332, 951–954,
459 doi:10.1126/science.1202131, 2011.
- 460 Karpechko, A. Y., Perlwitz, J., and Manzini, E.: A model study of tropospheric
461 impacts of the Arctic ozone depletion 2011, *J. Geophys. Res.*, 119, 7999–8014,
462 doi:10.1002/2013JD021350, 2014.
- 463 Kidston, J., Scaife, A. A., Hardiman, S. C., Mitchell, D. M., Butchart, N., Baldwin, M.
464 P., and Gray, L. J.: Stratospheric influence on tropospheric jet streams, storm
465 tracks and surface weather, *Nat. Geosci.*, 8, 433–440, doi:10.1038/NGEO2424,
466 2015.
- 467 Labitzke, K. and Naujokat, B.: The lower Arctic stratosphere in winter since 1952,
468 *Sparc Newsletter*, 15, 11–14, 2000.
- 469 Lau, K. M., Kim, K. M., and Shen, S. S.: Potential predictability of seasonal
470 precipitation over the U.S. from canonical ensemble correlation
471 predictions, *Geophys. Res. Lett.*, 29, 1–4, doi:10.1029/2001GL014263, 2002.
- 472 Lemke, P., Ren, R., and Alley, I.: The physical science basis. Contribution of Working
473 Group I to the fourth assessment report of the Intergovernmental Panel on
474 Climate Change, *Clim. Change*, 337–383, 2007.



- 475 Li, F., Vikhliav, Y. V., Newman, P. A., Pawson, S., Perlwitz, J., Waugh, D. W., and
476 Douglass, A. R.: Impacts of Interactive Stratospheric Chemistry on Antarctic and
477 Southern Ocean Climate Change in the Goddard Earth Observing System,
478 Version 5 (GEOS-5), *J. Climate*, 29, 3199–3218, doi:10.1175/JCLI-D-15-0572.1,
479 2016.
- 480 Lu, J., Deser, C., and Reichler, T.: Cause of the widening of the tropical belt since
481 1958, *Geophys. Res. Lett.*, 36, L03803, doi:10.1029/2008GL036076, 2009.
- 482 Manney, G. L., Santee, M. L., Rex, M., Livesey, N. J., Pitts, M. C., Veefkind, P., Nash,
483 E. R., Wohltmann, I., Lehmann, R., Froidevaux, L., Poole, L. R., Schoeberl, M.
484 R., Haffner, D. P., Davies, J., Dorokhov, V., Gernandt, H., Johnson, B., Kivi, R.,
485 Kyrö, E., Larsen, N., Levelt, P. F., Makshtas, A., McElroy, C. T., Nakajima, H.,
486 Parrondo, M. C., Tarasick, D. W., von der Gathen, P., Walker, K. A., and
487 Zinoviev, N. S.: Unprecedented Arctic ozone loss in 2011, *Nature*, 478, 469–475,
488 <https://doi.org/10.1038/nature10556>, 2011.
- 489 Manney, G. L. and Lawrence, Z. D.: The major stratospheric final warming in 2016:
490 dispersal of vortex air and termination of Arctic chemical ozone loss, *Atmos.*
491 *Chem. Phys.*, 16, 15371–15396, doi:10.5194/acp-16-15371-2016, 2016.
- 492 Marsh, D. R., Mills, M. J., Kinnison, D. E., Lamarque, J. F., Calvo, N., and Polvani, L.
493 M.: Climate Change from 1850 to 2005 Simulated in CESM1(WACCM), *J.*
494 *Climate*, 26, 7372–7391, doi:10.1175/JCLI-D-12-00558.1, 2013.
- 495 Marshall, G. J.: Trends in the Southern Annular Mode from observations and
496 reanalyses, *J. Climate*, 16, 4134–4143,



- 497 doi:10.1175/1520-0442(2003)016<4134:TITSAM>2.0.CO;2, 2003.
- 498 McLandress, C., Shepherd, T. G., Scinocca, J. F., Plummer, D. A., Sigmond, M.,
499 Jonsson, A. I., and Reader, M. C.: Separating the dynamical effects of climate
500 change and ozone depletion. Part II: Southern Hemisphere troposphere, *J.*
501 *Climate*, 24, 1850–1868, doi:10.1175/2010JCLI3958.1, 2011.
- 502 Min, S. K. and Son, S. W.: Multimodel attribution of the Southern Hemisphere
503 Hadley cell widening: Major role of ozone depletion, *J. Geophys. Res.*, 118,
504 3007–3015, doi:10.1002/jgrd.50232, 2013.
- 505 Namias, J.: Some causes of U.S. drought, *J. Clim. Appl. Meteorol.*, 22, 30–39,
506 doi:10.1175/1520-0450(1983)022<0030:Scousd>2.0.Co;2, 1983.
- 507 Neale, R. B., Richter, J., Park, S., Lauritzen, P. H., Vavrus, S. J., Rasch, P. J., and
508 Zhang, M. H.: The Mean Climate of the Community Atmosphere Model (CAM4)
509 in Forced SST and Fully Coupled Experiments, *J. Climate*, 26, 5150–5168,
510 doi:10.1175/JCLI-D-12-00236.1, 2013.
- 511 Pawson, S. and Naujokat, B.: The cold winters of the middle 1990s in the northern
512 lower stratosphere, *J. Geophys. Res.*, 104, 14209–14222,
513 doi:10.1029/1999JD900211, 1999.
- 514 Polvani, L. M., Waugh, D. W., Correa, G. J., and Son, S.-W.: Stratospheric ozone
515 depletion: The main driver of twentieth-century atmospheric circulation changes
516 in the Southern Hemisphere, *J. Climate*, 24, 795–812,
517 doi:10.1175/2010JCLI3772.1, 2011.
- 518 Ramaswamy, V., Schwarzkopf, M. D., and Randel, W. J.: Fingerprint of ozone



- 519 depletion in the spatial and temporal pattern of recent lower-stratospheric cooling,
520 Nature, 382, 616–618, doi:10.1038/382616a0, 1996.
- 521 Randel, W. J.: The Seasonal Evolution of Planetary-Waves in the
522 Southern-Hemisphere Stratosphere and Troposphere, Quarterly Journal of the
523 Royal Meteorological Society, 114, 1385–1409, doi:10.1002/qj.49711448403,
524 1988.
- 525 Randel, W. J. and Wu, F.: Cooling of the arctic and antarctic polar stratospheres due to
526 ozone depletion, J. Climate, 12, 1467–1479,
527 doi:10.1175/1520-0442(1999)012<1467:COTAAA>2.0.Co;2, 1999.
- 528 Randel, W. J. and Wu, F.: A stratospheric ozone profile data set for 1979-2005:
529 Variability, trends, and comparisons with column ozone data, J. Geophys. Res.,
530 112, D06313, doi:10.1029/2006JD007339, 2007.
- 531 Ravishankara, A. R., Turnipseed, A. A., Jensen, N. R., Barone, S., Mills, M., Howard,
532 C. J., and Solomon, S.: Do hydrofluorocarbons destroy stratospheric ozone?,
533 Science, 263, 71–75, doi:10.1126/science.263.5143.71, 1994.
- 534 Ravishankara, A. R., Daniel, J. S., and Portmann, R. W.: Nitrous oxide (N₂O): the
535 dominant ozone-depleting substance emitted in the 21st century, Science, 326,
536 123–125, doi:10.1126/science.1176985, 2009.
- 537 Reichler, T., Kim, J., Manzini, E., and Kroger, J.: A stratospheric connection to
538 Atlantic climate variability, Nat. Geosci., 5, 783–787, doi:10.1038/NGEO1586,
539 2012.
- 540 Russell, J. L., Dixon, K. W., Gnanadesikan, A., Stouffer, R. J., and Toggweiler, J. R.:



- 541 The Southern Hemisphere westerlies in a warming world: Propping open the
542 door to the deep ocean, *J. Climate*, 19, 6382–6390, doi:10.1175/JCLI3984.1,
543 2006.
- 544 Smith, K. L. and Polvani, L. M.: The surface impacts of Arctic stratospheric ozone
545 anomalies, *Environ. Res. Lett.*, 9, 074015, doi:10.1088/1748-9326/9/7/074015,
546 2014.
- 547 Solomon, S.: Antarctic ozone: Progress towards a quantitative understanding, *Nature*,
548 347, 354, doi:10.1038/347347a0, 1990.
- 549 Solomon, S.: Stratospheric ozone depletion: A review of concepts and history, *Rev.*
550 *Geophys.*, 37, 275–316, doi:10.1029/1999RG900008, 1999.
- 551 Son, S.-W., Tandon, N. F., Polvani, L. M., and Waugh, D. W.: Ozone hole and
552 Southern Hemisphere climate change, *Geophys. Res. Lett.*, 36, L15705,
553 doi:10.1029/2009GL038671, 2009.
- 554 Son, S.-W., Gerber, E. P., Perlwitz, J., Polvani, L. M., Gillett, N. P., Seo, K.-H., Eyring,
555 V., Shepherd, T. G., Waugh, D., Akiyoshi, H., Austin, J., Baumgaertner, A.,
556 Bekki, S., Braesicke, P., Brühl, C., Butchart, N., Chipperfield, M. P., Cugnet, D.,
557 Dameris, M., Dhomse, S., Frith, S., Garny, H., Garcia, R., Hardiman, S. C.,
558 Jöckel, P., Lamarque, J. F., Mancini, E., Marchand, M., Michou, M., Nakamura,
559 T., Morgenstern, O., Pitari, G., Plummer, D. A., Pyle, J., Rozanov, E., Scinocca, J.
560 F., Shibata, K., Smale, D., Teyssède, H., Tian, W., and Yamashita, Y.: Impact of
561 stratospheric ozone on Southern Hemisphere circulation change: A multimodel
562 assessment, *J. Geophys. Res.*, 115, D00M07, doi.org/10.1029/2010JD014271,



- 563 2010.
- 564 Thompson, D. W. J., Wallace, J. M., and Hegerl, G. C.: Annular modes in the
565 extratropical circulation. Part II: Trends, *J. Climate*, 13, 1018–1036,
566 doi:10.1175/1520-0442(2000)013<1018:AMITEC>2.0.CO;2, 2000.
- 567 Thompson, D. W. J. and Solomon, S.: Interpretation of recent Southern Hemisphere
568 climate change, *Science*, 296, 895–899, doi:10.1126/science.1069270, 2002.
- 569 Thompson, D. W. J., Solomon, S., Kushner, P. J., England, M. H., Grise, K. M., and
570 Karoly, D. J.: Signatures of the Antarctic ozone hole in Southern Hemisphere
571 surface climate change, *Nature Geosci.*, 4, 741–749, doi:10.1038/NGEO1296,
572 2011.
- 573 Ting, M. and Wang, H.: Summertime US Precipitation Variability and Its Relation
574 to Pacific Sea Surface Temperature, *J. Climate*, 10, 1853–1873,
575 doi:10.1175/1520-0442(1997)010<1853:SUSPVA>2.0.CO;2, 1997.
- 576 Tung, K. K.: On the Relationship between the Thermal Structure of the Stratosphere
577 and the Seasonal Distribution of Ozone, *Geophys. Res. Lett.*, 13, 1308–1311,
578 doi:10.1029/GL013i012p01308, 1986.
- 579 Wang, F., Yang, S., Higgins, W., Li, Q. P., and Zuo, Z. Y.: Long-term changes in total
580 and extreme precipitation over China and the U.S. and their links to
581 oceanic-atmospheric features, *Int. J. Climatol.*, 34, 286–302,
582 doi:10.1002/joc.3685, 2014.
- 583 Wang, H. and Ting, M. F.: Covariabilities of winter US precipitation and Pacific Sea
584 surface temperatures, *J. Climate*, 13, 3711–3719,



- 585 doi:10.1175/1520-0442(2000)013<3711:Cowusp>2.0.Co;2, 2000.
- 586 Wang, L., Ting, M., Kushner, P. J.: A robust empirical seasonal prediction of winter
587 NAO and surface climate, *Sci. Rep.*, 7, 279, 2017.
- 588 Waugh, D. W., Garfinkel, C. I., and Polvani, L. M.: Drivers of the Recent Tropical
589 Expansion in the Southern Hemisphere: Changing SSTs or Ozone Depletion?, *J.*
590 *Climate*, 28, 6581–6586, doi:10.1175/JCLI-D-15-0138.1, 2015.
- 591 WMO: Scientific Assessment of Ozone Depletion: 2010. WMO Tech. Note 52, World
592 Meteorological Organization, Geneva, Switzerland, 516 pp., 2011.
- 593 Xie, F., Li, J., Tian, W., Fu, Q., Jin, F.-F., Hu, Y., Zhang, J., Wang, W., Sun, C., Feng,
594 J., Yang, Y., and Ding, R.: A connection from Arctic stratospheric ozone to El
595 Niño-Southern Oscillation, *Environ. Res. Lett.*, 11, 124026,
596 doi:10.1088/1748-9326/11/12/124026, 2016.
- 597 Xie, F., Li, J., Zhang, J., Tian, W., Hu, Y., Zhao, S., Sun, C., Ding, R., Feng, J., Yang,
598 Y.: Variations in North Pacific sea surface temperature caused by Arctic
599 stratospheric ozone anomalies, *Environ. Res. Lett.*, 12, 114023,
600 doi:10.1088/1748-9326/aa9005, 2017a.
- 601 Xie, F., Zhang, J., Sang, W., Li, Y., Qi, Y., Sun, C., and Shu, J.: Delayed effect of
602 Arctic stratospheric ozone on tropical rainfall, *Atmos. Sci. Lett.*, 18, 409–416,
603 2017b.
- 604 Xie, F., Ma, X., Li, J., Huang, J., Tian, W., Zhang, J., Hu, Y., Sun, C., Zhou, X., Feng,
605 J., Yang, Y.: An advanced impact of Arctic stratospheric ozone changes on spring
606 precipitation in China, 2018. (Submitted to *Clim. Dyn.*)



- 607 Yin, J. H.: A consistent poleward shift of the storm tracks in simulations of 21st
608 century climate, *Geophys. Res. Lett.*, 32, L18701, doi:10.1029/2005GL023684,
609 2005.
- 610 Zhang, J. K., Tian, W. S., Chipperfield, M. P., Xie, F., and Huang, J. L.: Persistent
611 shift of the Arctic polar vortex towards the Eurasian continent in recent decades,
612 *Nat. Clim. Change.*, 6, 1094–1099, doi:10.1038/nclimate3136, 2016.



613 **Table 1.** CESM-WACCM4 experiments with various specified ozone and SST
 614 forcing.

Exp ^{*1}	Specified ozone and SST forcing	Other forcing
R1	Time-slice run as the control experiment used case F_2000_WACCM_SC. The specified ozone forcing is a 12-month cycle of monthly ozone averaged from 1995 to 2005. The specified SST forcing is a 12-month cycle of monthly SST averaged from 1995 to 2005.	Fixed solar constant, fixed greenhouse gas (GHG) values (averages of emissions scenario A2 of the Intergovernmental Panel on Climate Change (WMO, 2003) over the period 1995–2005), volcanic aerosols (from the Stratospheric Processes and their Role in Climate (SPARC) Chemistry–Climate Model Validation (CCMVal) REF-B2 scenario recommendations), and QBO phase signals with a 28-month zonal wind fixed cycle.
R2	Same as R1, except that the March ozone in the region 30°–90°N at 300–30 hPa ^{*2} is decreased by 15% compared with R1.	Same as R1
R3	Same as R1, except that March ozone in the region 30°–90°N at 300–30 hPa is increased by 15% compared with R1.	Same as R1
R4	Same as R2, except that a SST anomalies in the region 0°–70°N and 120°E–90°W related to negative ASO anomalies ^{*3} is added in the SST forcing in April.	Same as R1
R5	Same as R3, except that a SST anomalies in the region 0°–70°N and 120°E–90°W related to positive ASO anomalies ^{*4} is added in the SST forcing in April.	Same as R1
R6	Same as R1, except that a SST anomalies in the region 0°–70°N and 120°E–90°W related to negative ASO anomalies ^{*3} is added in the SST forcing in April.	Same as R1



	Same as R1, except that a SST anomalies in the region 0° – 70° N and	
R7	120° E– 90° W related to positive ASO anomalies ^{*4} is added in the SST forcing in April.	Same as R1

615 ^{*1}Integration time for time-slice runs is 33 years.

616 ^{*2}To avoid the effect of the boundary of ozone change on the Arctic stratospheric
617 circulation simulation, the replaced region (30° – 90° N, 300–30 hPa) was larger than
618 the region used to define the ASO index (60° – 90° N, 150–50 hPa).

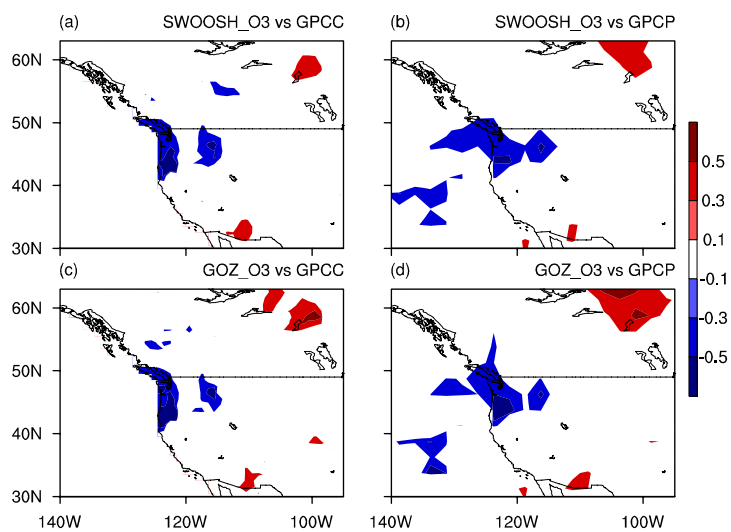
619 ^{*3}For SST anomalies, see Fig. 12a.

620 ^{*4}For SST anomalies, see Fig. 12b.



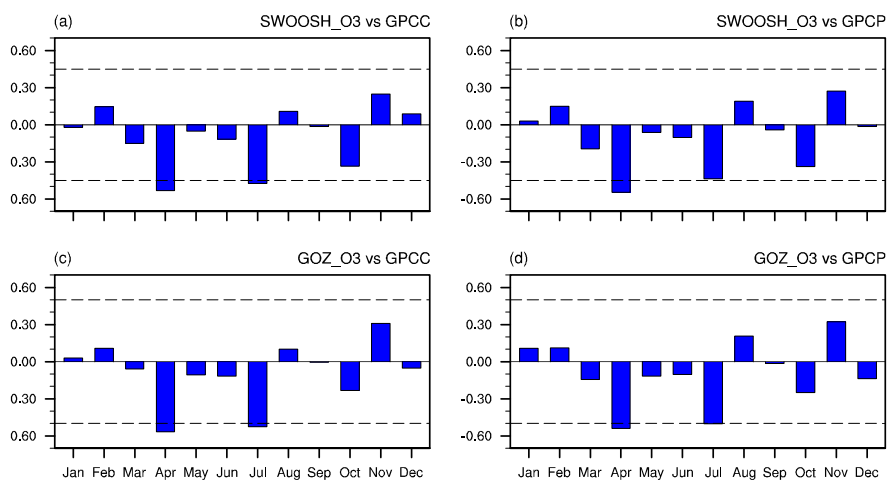
621 **Table 2.** Selected positive and negative years for March ASO anomaly events based
622 on SWOOSH data for the period 1984–2016. Positive and negative March ASO
623 anomaly events are defined using a normalized time series of March ASO variations
624 from 1984 to 2016. Values larger than 1 standard deviation are defined as positive
625 March ASO anomaly events, and those below -1 standard deviation are defined as
626 negative March ASO anomaly events.

Positive March ASO anomaly events	Negative March ASO anomaly events
1998, 1999, 2001, 2004, 2010	1993, 1995, 1996, 2000, 2011



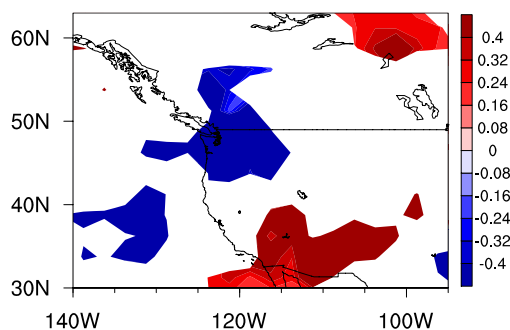
627

628 **Figure 1.** Correlation coefficients between March ASO and April precipitation
 629 variations calculated from SWOOSH (a, b) and GOZCARDS (c, d) ozone, and GPCP
 630 (a, c) and GPCP (b, d) rainfall for the period 1984–2016. Only regions above the 90%
 631 confidence level are colored. The long-term linear trend and seasonal cycle in all
 632 variables were removed before the correlation analysis.



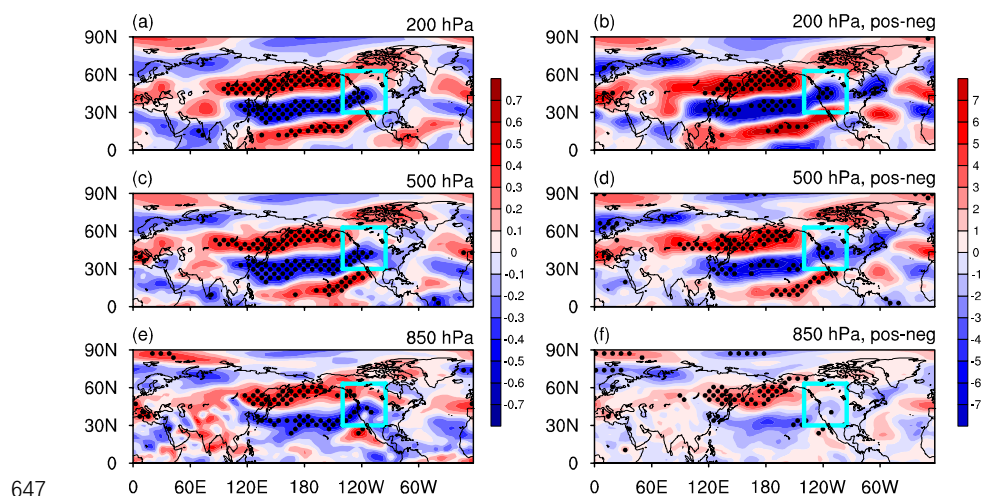
633

634 **Figure 2.** (a) Correlation coefficients between March ASO index and precipitation
635 anomalies in the northwestern US (43° – 50° N, 115° – 130° W) for each month
636 calculated from SWOOSH (a, b) and GOZCARDS (c, d) ozone, and GPCP (a, c) and
637 GPCP (b, d) rainfall for the period 1984–2016. The long-term linear trend and
638 seasonal cycle were removed from the original datasets before calculating the
639 correlation coefficients.



640

641 **Figure 3.** Differences in composite April precipitation (mm/day, from GPCP)
642 anomalies in the US between positive and negative ASO anomaly events (from
643 SWOOSH data) for 1984–2016. Only regions above the 90% confidence level are
644 colored. See Table 2 for the definition of positive and negative March ASO anomaly
645 events for composite analysis. Before performing the composite analysis, the seasonal
646 cycle and linear trend were removed from the original precipitation dataset.

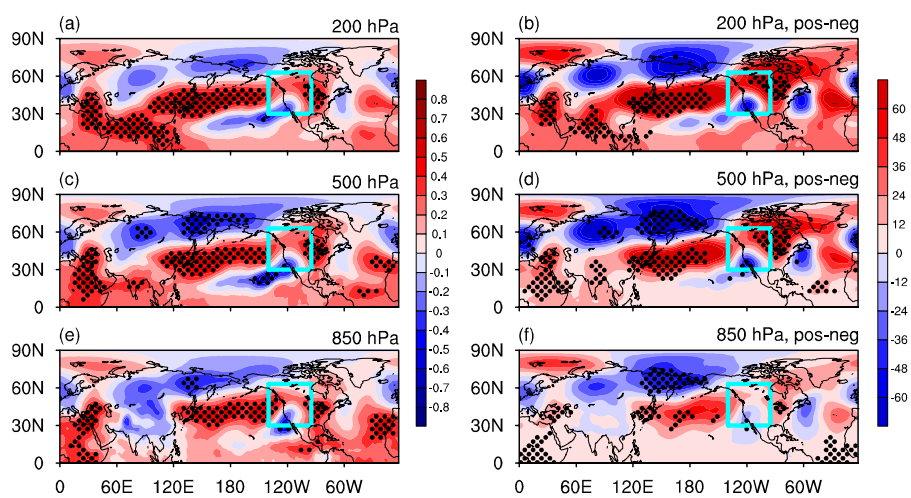


647

648 **Figure 4.** Correlation coefficients between March ASO index and April zonal wind
649 variations (m/s, from NCEP2) from 1984 to 2016 at 200 hPa (a), 500 hPa (c), and 850
650 hPa (e). Differences in composite April zonal wind (m/s) anomalies between positive
651 and negative ASO anomaly events are shown at 200 hPa (b), 500 hPa (d), and 850 hPa
652 (f). Dots denote significance at the 90% confidence level, according to Student's *t*-test.
653 Blue square is the area shown in Fig. 1. Before performing the analysis, the seasonal
654 cycle and linear trend were removed from the original datasets. Selected ASO
655 anomalous events are based on Table 2.

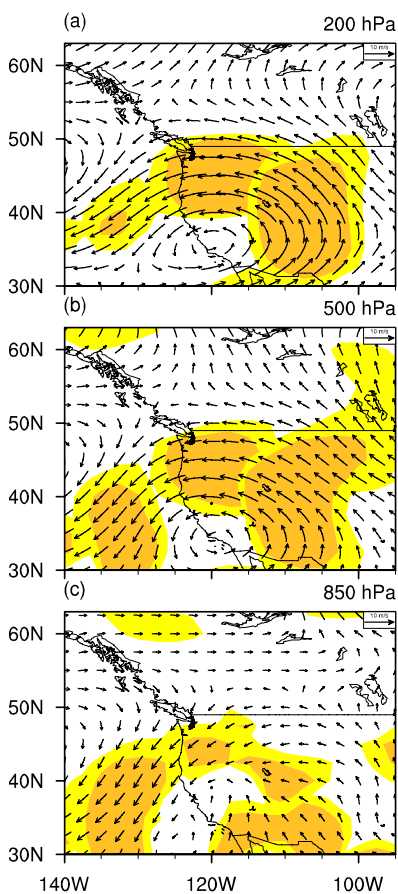


656



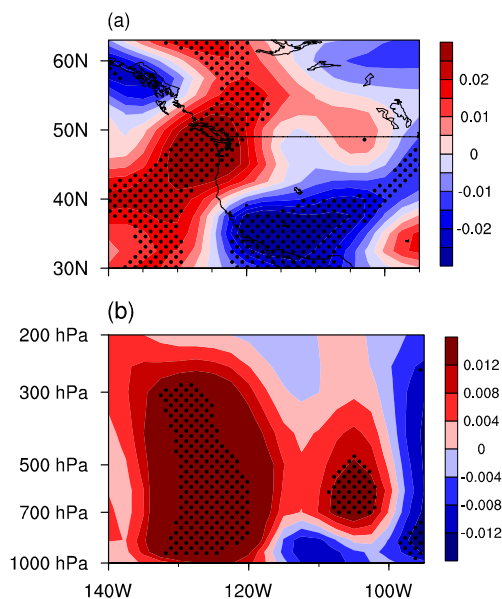
657

658 **Figure 5.** Same as Fig. 4, but for geopotential height (m).



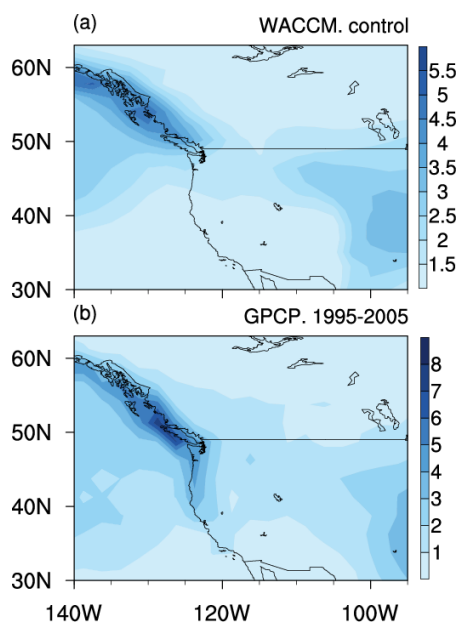
659

660 **Figure 6.** Differences in composite April winds (vectors, m/s, from NCEP2) between
 661 positive and negative ASO anomaly events at 200 hPa (a), 500 hPa (b), and 850 hPa
 662 (c) for 1984–2016. Colored regions are statistically significant at the 90% (light
 663 yellow) and 95% (dark yellow) confidence levels. The seasonal cycle and linear trend
 664 were removed from the original dataset. The ASO anomaly events are selected based
 665 on Table 2.



666

667 **Figure 7.** (a) Longitude–latitude cross-section of differences in composite April
668 vertical velocity anomalies (averaged over 1000–500 hPa) between positive and
669 negative ASO anomaly events for 1984–2016. (b) Longitude–height cross-section of
670 differences in composite April vertical velocity anomalies (averaged over 43°–50°N)
671 between positive and negative ASO anomaly events from 1984 to 2016. Dots denote
672 significance at the 90% confidence level. Before performing the analysis, the seasonal
673 cycle and linear trend were removed from the original dataset. The ASO anomaly
674 events are selected based on Table 2. The vertical velocity (Pa/s) dataset is from
675 NCEP2.

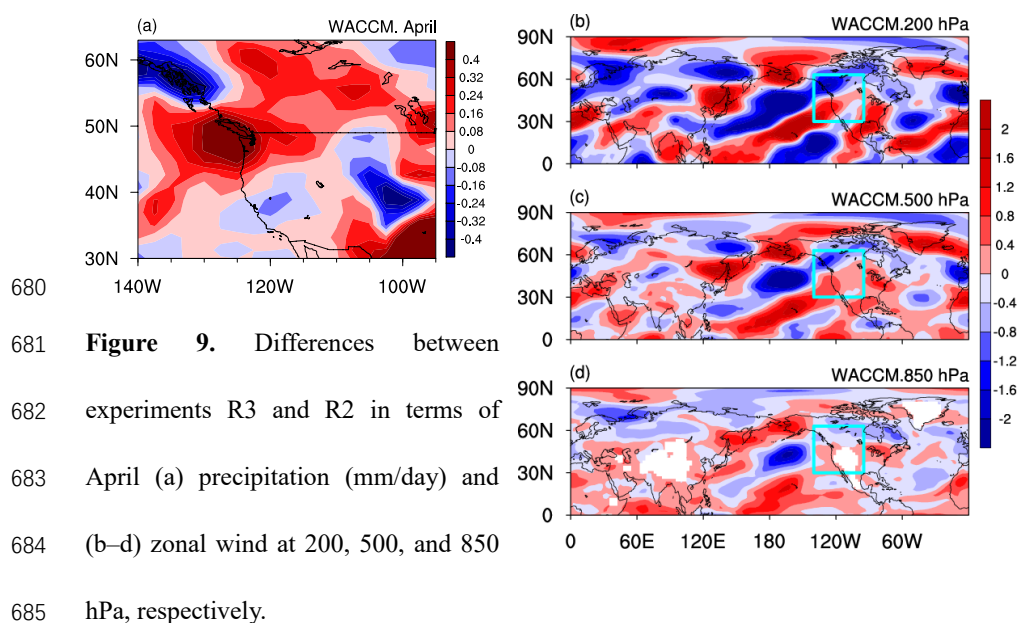


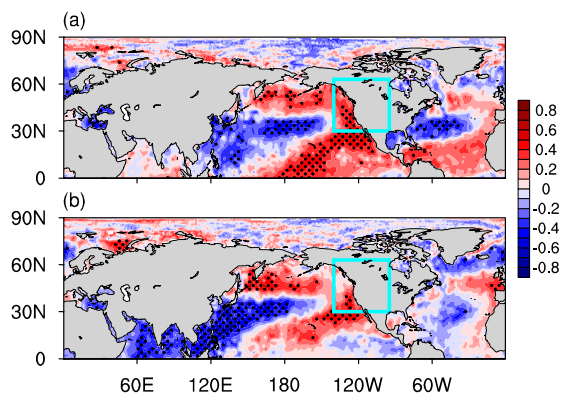
676

677 **Figure 8.** (a) Spatial distribution of April precipitation (mm/day) climatology in the

678 control experiment (R1). (b) Same as (a), but precipitation from the GPCP for the

679 period 1995–2005. For details of specific experiments, see Table 1.





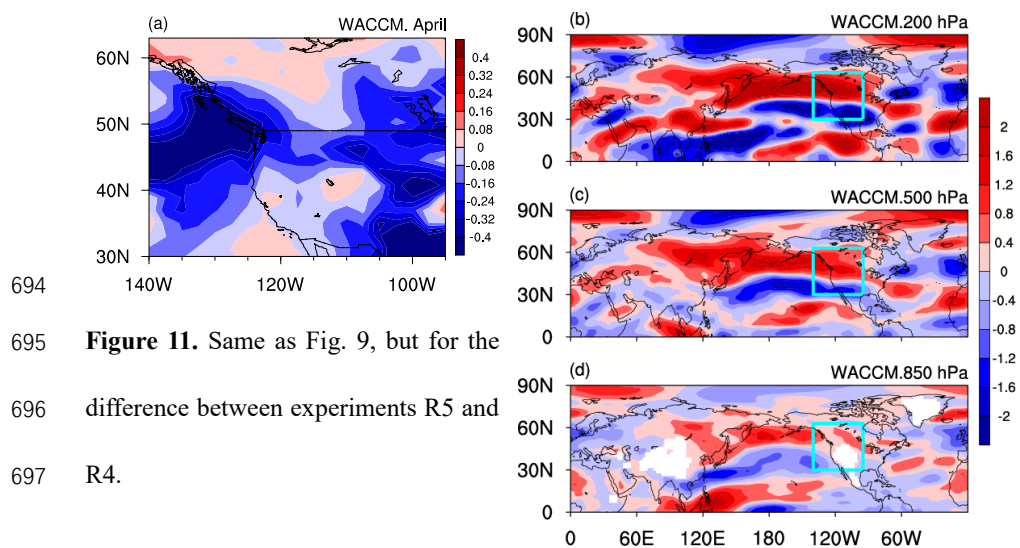
686

687 **Figure 10.** (a) Correlation coefficients between regional precipitation (43° – 50° N,688 115° – 130° W) and SST variations in April for 1984–2016. (b) Correlation coefficients689 between March ASO ($\times -1$) and April SST variations for 1984–2016. Dots denote690 significance at the 90% confidence level, according to Student's t -test. Before

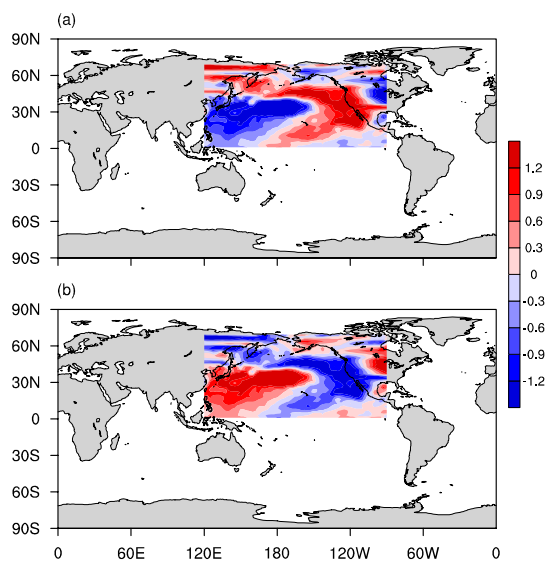
691 performing the analysis, the seasonal cycle and linear trend were removed from the

692 original data. ASO data are from SWOOSH, precipitation from NCEP2, and SST

693 from HadSST.



695 **Figure 11.** Same as Fig. 9, but for the
696 difference between experiments R5 and
697 R4.



698

699 Figure 12. (a) Composite SST anomalies during negative ASO anomaly events. (b)

700 Composite SST anomalies during positive ASO anomaly events. The ASO anomaly

701 events are selected based on Table 2. SST data are from CESM SST forcing data.

